Fragmentation of stretched spin strength in $N = Z$ sd-shell nuclei

J. A. Carr
Supercomputer Computations Research Institute, Florida State University, Tallahassee, Florida 32306

S. D. Bloom
Lawrence Livermore National Laboratory, Livermore, California 94550

F. Petrovich and R. J. Philpott
Department of Physics, Florida State University, Tallahassee, Florida 32306

(Received 1 November 1991)

Calculations have been performed to explore the effect of configuration mixing in a large basis on the fragmentation of "stretched" $M6$ strength in the sd-shell nuclei ^{20}Ne, ^{24}Mg, ^{28}Si, ^{32}S, and ^{36}Ar. This work elaborates on results for ^{28}Si given previously, extends those calculations to neighboring $N = Z$ nuclei with the same basis restriction (one particle in the $1f_{7/2}$ orbit and up to four particles in the $1d_{3/2}$ orbit) used in that earlier paper, and examines all self-conjugate sd-shell nuclei in a basis with one particle in the $1f_{7/2}$ orbit and unrestricted occupancy of the sd-shell orbits. It is found that configuration mixing in a large basis reproduces interesting features of the spectrum for ^{28}Si and ^{32}S and gives an improved description of other properties of the observed 6^- states, but fails to describe the observed spectrum in ^{24}Mg. Emphasis is placed on the location of additional observable fragments of the $M6$ response.

PACS number(s): 21.10.Re, 27.30.+t, 21.60.Cs, 23.20.Js

I. INTRODUCTION

In an earlier paper [1] we reported evidence that the distribution of stretched spin strength that has been the subject of much experimental and theoretical activity [2–12] could be explained, in the case of 6^- states in the ^{28}Si nucleus, as a consequence of fragmentation in a suitably large shell-model basis. In this paper we provide more information on those calculations and present new results for the other $N = Z$ sd-shell nuclei that reinforce our conclusion that fragmentation is the principal source for the reduction, relative to single-particle estimates, of observed stretched spin strength.

"Stretched" particle-hole states, for the even-even nuclei typically studied, have negative parity and total angular momentum $J = j_h + j_p$ that is the fully aligned sum of the maximum possible hole and particle angular momenta, $j_h = \ell_h + \frac{1}{2}$ and $j_p = \ell_p + \frac{1}{2}$, in the valence shell and the shell lying immediately above it, respectively. In the sd-shell nuclei of interest here, these are 6^- states. To be more precise, it is the unique $(1f_{7/2}1d_{5/2}^{-1})$ configuration that is "stretched" and not the 6^- states themselves. (Our language tends to reflect early expectations that this stretched configuration would appear as a single state [3].) These 6^- states have the property that the strength observed via one-step inelastic-scattering reactions is due only to the single stretched component of its wave function, whether it appears as a single state or is fragmented by configuration mixing, when interpreted within a $(0+1)\hbar\omega$ model space [4–8].

This crucial property, that excitation of any 6^- state via a one-step $M6$ transition from an sd-shell 0^+ ground state proceeds through the stretched configuration, means scattering experiments can be used to map out the distribution of this unique configuration among all the 6^- states. Further, interpretation of such inelastic-scattering data is simplified because this configuration gives rise to a single spin transition density, ρ^S_{JL} with $J = 6$, $L = 5$, and $S = 1$ for an $M6$ excitation, that is the sole common source for the cross section, given schematically [11] in the plane-wave approximation by

$$\frac{d\sigma}{d\Omega}^{\mathrm{PWBA}} = 4\pi \left(\frac{\mu}{2\pi\hbar^2}\right)^2 (2J+1) \left|\bar{t}_s\right|^2 \left|\rho^S_{JL}\right|^2 , \tag{1}$$

measured in electron, nucleon, and pion inelastic scattering reactions. In this expression, $\bar{t}_s$ is a probe-dependent interaction strength [11] and μ is the reduced total energy of the projectile. (These statements are based on the assumption that $3\hbar\omega$ states do not intrude [4–8] and that exchange nonlocalities can be modeled with a single effective coupling strength [13]; note that the former assumption remains valid even in the presence of configuration mixing as emphasized in Ref. [8].) This is to be contrasted with the situation for $M1$ excitations where the presence of convection currents (see Ref. [11] for the relevant version of Eq. (1)) complicates the analysis of scattering data.

The fact that a single transition density drives the excitation of these states in inelastic-scattering reactions, regardless of the probe used, provides us with a very

powerful tool. Because magnetic electron scattering is mainly (by a factor of 28) sensitive to isovector excitations, we can employ it to deduce the strength of those excitations with great precision. Hadronic probes can then be calibrated against the isovector excitations and subsequently used to deduce the strength for isoscalar transitions. Experiments with a variety of intermediate energy probes give consistent results for the spin strength attributable to the "stretched" configuration [5–12], verifying this model.

The observed strength is typically a small fraction of the strength expected for a pure particle-hole excitation—generally less than $\frac{1}{3}$ for isoscalar excitations and less than $\frac{1}{2}$ for isovector excitations. What this means, of course, is that the stretched configuration makes up only a small fraction of the total wave function of the so-called "stretched state." It is this depletion of strength that we wish to understand, because it provides information on the spin-dependent parts of the effective interaction in nuclei.

Since the wave function is normalized, it must be that the "missing strength" has been displaced by other configurations. A convenient language for discussion of this redistribution of strength can be obtained by expressing the closure relation schematically as

$$|M6\rangle\langle M6| + |1\hbar\omega\rangle\langle 1\hbar\omega| + |C\rangle\langle C| + |\Delta\rangle\langle\Delta| = 1,$$

where $|M6\rangle$ is the stretched $1\hbar\omega$ configuration, $|1\hbar\omega\rangle\langle 1\hbar\omega|$ implies a summation over the set of all other possible 6^- configurations in a $1\hbar\omega$ basis, $|C\rangle\langle C|$ implies a summation over the remaining ($\geq 3\hbar\omega$) core excitations, and we have included $|\Delta\rangle\langle\Delta|$, indicating a summation over all 6^- configurations in the non-nucleonic sector, such as Δ-hole states, that have been considered by some workers. Each term in this expression is thus a projection operator for the key elements that enter various structure calculations.

The reduction in observed strength is generally referred to as "quenching" in the literature, but we prefer to reserve "quenching" for the specific case where strength is removed by mixing with states far away in the spectrum (such as is the case for Δ-hole states, which lie hundreds of MeV above the states of interest, or highly excited core polarization contributions) so there is no expectation that the displaced strength will be seen in the region of excitation being studied experimentally. In that case, use of "quenched" effective operators makes sense. We prefer to use the term "fragmentation" to describe the situation where strength is redistributed by mixing with nearby configurations, as when mixing with $|1\hbar\omega\rangle$ configurations is considered, so there is a chance that other fragments of the stretched configuration might be observable. In the latter case, the spectral distribution of strength, and not just an overall scale factor for the strongest state, is of interest and can give us important information about the mixing that took place.

The effects of non-nucleonic degrees of freedom, implied by the $|\Delta\rangle\langle\Delta|$ projection operator in the expression above, are largest for $M1$ and Gamow-Teller (GT) transitions. Calculations [14–16] indicate that non-nucleonic degrees of freedom such as the Δ might give up to 20% contributions to the transition matrix elements in those cases. These same models [14–16] indicate negligible corrections to stretched transitions due to Δ degrees of freedom. We will not consider them further.

Many studies have used the perturbative approach whereby particle-hole excitations involving high-lying shells, the space denoted by $|C\rangle$ above, polarize the core and reduce the one-step $M6$ transition rate. However, when realistic interactions are employed, these core-polarization effects produce only half of the required strength reduction [17–24]. Further, the core-polarization corrections tend to be nearly identical for $T = 0$ and $T = 1$ excitations [22, 24], as emphasized in Ref. [7], while the reduction in strength is markedly asymmetric. These arguments indicate that "quenched" effective operators arising from the omission of $|C\rangle$ wave-function components from the Hilbert space used for our calculations cannot be the dominant source of the observed strength reduction.

Studies also have been made where the nonperturbative effects of valence-space configuration mixing were estimated in a rotational model [25–27]. This approach has the advantage that important ground-state correlations (including those from the $|1\hbar\omega\rangle$ space and some from the $|C\rangle$ space) are included in a compact fashion, which makes the calculations more practical in heavier nuclei than the corresponding shell-model calculation. From our point of view, it is also important that these models make predictions for the spectrum of the stretched strength. The location of potentially observable weak fragments of the stretched configuration provides an important test of any configuration-mixing model.

The expectation that valence-space configuration-mixing effects are primarily responsible for the observed depletion of "stretched" spin strength has motivated several shell-model studies of stretched transitions within the $|1\hbar\omega\rangle$ space. Initial studies [28–30] were able to explain only about half of the depletion of strength, with the exception of some studies of "stretched" 4^- states in p-shell nuclei where the small basis size allowed full $(0 + 1)\hbar\omega$ calculations. In the ^{12}C case examined by van Hees and Glaudemans [30], the $T = 1$ state is predicted to contain 58% of the extreme single-particle-hole model (ESPHM) estimate and the $T = 0$ state is fragmented into several states with the strongest containing 40% of the ESPHM estimate. These compare favorably with the 32–40% fraction of the ESPHM seen experimentally for the $T = 1$ state [31], with the exact number depending on whether one deals with the known isospin mixing [32], and the (38 ± 11)% seen experimentally for the T=0 state [31, 33]. Calculations by Millener [31], based on the work of Ref. [28], give similar results. We should add that the work of Yokoyama and Horie [23] indicates that core polarization (i.e., adding the $|C\rangle$ space perturbatively) can explain much of the remaining discrepancy between the isovector strength predicted by van Hees and Glaudemans and that observed experimentally; however, Ref. [23] did not examine the isoscalar states, where no additional reduction seems necessary. The point is that core polarization is expected to provide

a small, perturbative correction to the spectrum obtained in the $1\hbar\omega$ space. We emphasize that it is this spectrum, which shows the location of the "missing" fragments of $M6$ strength, that is most crucial to understanding the physics of these states.

The challenge has been to extend such relatively complete calculations to the *sd* shell (and beyond) so that systematic comparisons can provide additional tests of the model. In an earlier shell-model study in the *sd* shell, Amusa and Lawson [29] (hereinafter to be called AL) examined the effect of limited configuration mixing on several aspects pertaining to the single particle transition $1d_{5/2} \rightarrow 1f_{7/2}$ in ^{28}Si. Liu and Zamick [26] have made related studies using the rotational model with Coriolis mixing. In the work of AL, significant improvement in the inelastic-scattering cross sections and transfer-reaction spectroscopic factors for the lowest $T = 0$ and $T = 1$ 6^- states and the $B(M1)$ transition rate between them was found when the zero-order (pure particle-hole) prediction based on the $(1d_{5/2})^{12} \rightarrow (1d_{5/2})^{11}(1f_{7/2})$ transition is extended to include the $1s_{1/2}$ level in the core.

This limited success, and the remaining discrepancies between their findings and the experimental limits on the full spectrum of 6^- strength determined from pion, proton, and electron scattering, motivated us to extend the model space further by allowing up to 4 particles to populate the $1d_{3/2}$ level. This basis contains 75% of the 6^- states in a full $(sd)^{11}f_{7/2}$ basis for ^{28}Si, and thus gives a good measure of the results to be expected from full $(0+1)\hbar\omega$ configuration mixing in *sd*-shell nuclei. Here we report further on that work [1], extend it to provide more systematic results that include the neighboring $N = Z$ nuclei of ^{32}S (some of which were presented in Ref. [34]) and ^{24}Mg within the same basis truncation, and show results for the full *sd* space in calculations for all $N = Z$ *sd*-shell nuclei [35]. We restrict our discussion to self-conjugate nuclei to avoid the additional complications produced by neutron-proton mixing.

In the remainder of this paper we first describe, in more detail than was possible in our previous paper [1], the model and methods used to calculate the $M6$ strength distribution and other properties of the 6^- states in these *sd*-shell nuclei. We then present results for each of the nuclei in turn and close with a discussion of their implications for future work in this area.

II. METHODS

The calculations described in this work were performed in the bases

$$(d_{5/2}, s_{1/2})^{m-n}\ d^n_{3/2}$$

and

$$(d_{5/2}, s_{1/2})^{m-n-1}\ d^n_{3/2}\ f_{7/2},$$

where $m = A - 16$ and $0 \leq n \leq n_{\max}$, with $n_{\max} = 0$, 4, and 8 used as different basis restrictions. We use a Hamiltonian that consists of the Wildenthal (BHW) effective Hamiltonian for the full *sd* shell [36] and the "best-fit" Shiffer-True (ST) central spin-dependent interaction, constructed from the second set of entries in Table XVI of Ref. [37] with $r_1 = 1.45$ fm and $r_2 = 2.0$ fm, to connect the *sd* and *f* configurations. The latter is evaluated for harmonic-oscillator radial functions using $\nu = 0.293$, corresponding to a size parameter $b = 1.847$ fm, to be consistent with previous work [29]. The $f_{7/2}$ single-particle energy (s.p.e.) is adjusted to give the correct excitation energy for the lowest 6^- $T = 0$ state in ^{28}Si. (This makes that s.p.e. depend slightly on the basis truncation used; its value is about 6.8 MeV.)

We also have repeated the AL calculation for ^{28}Si, corresponding to $n_{\max} = 0$ in our notation above, and did a similar calculation for the ^{24}Mg case they did not do. This calculation requires use of a Hamiltonian consisting of the Wildenthal, McGrory, Halbert, and Glaudemans (WMHG) effective interaction appropriate to the $d_{5/2}, s_{1/2}$ space [38] plus the same ST central spin-dependent interaction to connect the two spaces. A significantly different $f_{7/2}$ s.p.e. is required to locate the lowest $T = 0$ state correctly for this case. (Calibrating on the lowest *isovector* state would reduce the need for this big change between the AL case and the present work, since the isovector eigenenergy is less affected by the mixing, but we choose to stay with the AL procedure, for now.) The WMHG/ST Hamiltonian is used only to explore the systematic trends attributable to the change in basis size that was the main point of our earlier paper.

Since our main concern is with the depletion of strength seen in inelastic scattering, we are interested in matrix elements

$$Z_T = \langle \Psi_{6^-,T} \| A^6_{T,0}(f_{7/2}, d_{5/2}) \| \Psi_{\text{g.s.}} \rangle \tag{2}$$

(reduced in spin-space only), the Raynal Z coefficient [39], of the operator

$$A^{6,M}_{T,T_z}(j_f, j_i) = \left[a^\dagger_{j_f m_f, t_{z_f}} a_{j_i, m_i, t_{z_i}} \right]^{6,M}_{T,T_z} \tag{3}$$

for the full spectrum of 6^- states in ^{28}Si. In this expression, $a^\dagger$ creates a particle, a annihilates one, and the square brackets indicate coupling to the total angular momentum 6 and isospin T with the usual factors to ensure the correct rotational properties [39]. Note that $\Psi_{\text{g.s.}}$ has $J^\pi = 0^+$ and $T = 0$ so the A^6_T operator connects to a state with the isospin T carried by the operator.

The simplicity of the "stretched" states guarantees that the inelastic-scattering cross section is proportional to Z^2_T for all probes considered, but the large number of possible states (up to 82 000 in our largest basis) makes it impractical to evaluate Z^2 explicitly for each eigenstate of the model system. The Lanczos algorithm provides a convenient alternative [40], since it obviates the need to pursue a full diagonalization in this space but, as Whitehead [41] has shown, still gives a description of the distribution of strength as a function of energy accurate to the $(2N - 1)$th moment after N Lanczos iterations. This algorithm also converges fastest for the lowest-lying states, so we get "sharp" states for the yrast $T = 0$ and $T = 1$ levels observed experimentally.

The specific procedure is to start from a good ground

state for the nucleus obtained by diagonalization within the (relatively small) *sd*-shell basis. Then we form the "collective vector" [42] for the 6^- state of isospin T defined by

$$|\chi_T\rangle = A^{6,6}_{T,0}|\Psi_{\text{g.s.}}\rangle \tag{4}$$

that contains all of the $M6$ strength in this basis and thus determines

$$\Sigma = \langle\chi_T|\chi_T\rangle \ , \tag{5}$$

a "sum rule" that gives the integral of Z^2_T over all $M6$ transitions for a given isospin transfer in our model space; the value of Σ is determined by the occupancy of the $d_{5/2}$ orbit in the ground state. (Σ is independent of T.) Zamick [25] has pointed out that the reduction of Σ from unity (for ^{28}Si) is a natural consequence of deformation of the core and the resultant depletion of the $d_{5/2}$ orbit. The "collective vector" is used as the first Lanczos vector

$$|L_1\rangle = |\chi_T\rangle \ \langle\chi_T|\chi_T\rangle^{-1/2}, \tag{6}$$

making it trivial to follow the fragmentation of this specific configuration. This follows since we can compute Z^2 directly and cheaply from Σ and the coefficient of this vector–a clear measure of its fragmentation–in each *pseudo*eigenvector at any stage of the calculation. (This method is simplest to use for an $I = T = 0$ ground state such as we consider here.) Specifically, when we find the *pseudo*eigenstates

$$|E_i\rangle = \sum_{j=1}^{N} a_j(i) \ |L_j\rangle \tag{7}$$

after N iterations of the Lanczos algorithm, it is easy to compute the spectrum from

$$\begin{aligned} Z^2_T(i) &= \langle E_i|A^{6,6}_{T,0}|\Psi_{\text{g.s.}}\rangle^2 \\ &= \langle E_i|\chi_T\rangle^2 \\ &= |a_1(i)|^2 \ \Sigma \end{aligned} \tag{8}$$

and the eigenenergies E_i and widths

$$\Gamma = \langle(H - \langle H\rangle)^2\rangle^{1/2} \ . \tag{9}$$

The theorem mentioned above guarantees [41] that the resulting spectrum has the same moments as the exact spectrum up to E^{2N-1}.

At this point we wish to call the reader's attention to some key differences between this method and that used in more familiar shell-model structure calculations. Normally one defines a model space and diagonalizes the Hamiltonian to obtain the full spectrum of eigenstates and their associated many-particle eigenvectors, subject only to the limitations of the model used. We cannot do this for the problem under study, and we use the jargon *pseudo*eigenstates to indicate that only part, albeit the most important part, of the exact *model* eigenvector is included in our answer. Unimportant, in this context, means that the coefficients for the many Lanczos basis vectors that would be added to the expression of Eq. (7) for the low-lying states, if we were to iterate to completion, are extremely small. For example, the 24th vector only contributes $\sim 10^{-7}$ to the magnitude of the yrast $T = 0$ state for ^{28}Si. The width Γ defined in Eq. (9) results from the fact that the *pseudo*eigenstate in Eq. (7) is not an eigenstate of the model H.

We use the spectra generated by the procedure described above as a compact means of displaying the scattering strength expected for the lowest 6^- states as a result of using different model space truncations, as well as the distribution of $M6$ strength at high E_x that results from the fragmentation of the single-particle configuration. Following the Livermore approach [42], the curves in the figures are based on the magnitude of Z^2 for the individual pseudoeigenstates spread by a Gaussian of width Γ or 100 keV, whichever is larger. Such a curve is proportional to the inelastic-scattering cross section at the peak of the angular distribution, except one must keep in mind that the broad bumps represent a large number of small states with the given distribution. It is probable that the strength will actually appear spread over all of these states if the Lanczos iterations were carried to convergence, but we have no way to know whether it actually appears in a few stronger states with the same moments.

This ambiguity regarding the location of the actual eigenstates leads to some difficulties when we wish to compare our predictions to the observed spectrum. However, the states at higher E_x are unbound so their large real widths tend to mask this problem. (Of course, calculations in that domain should also include explicit coupling to the continuum [43]. Such work is beyond the scope of the current project.) In addition, we typically have experimental data for the yrast states where our calculation is sufficiently converged so that only a small energy error ($\Gamma \lesssim 10^{-3}$ MeV) remains from the fact that the wave function is not quite a proper eigenstate of the model Hamiltonian. The artificial width of 100 keV keeps the spectrum looking normal, and we place the "data points" at a height corresponding to the top of a Gaussian of this same 100 keV width and an area equal to the measured strength. The reader should compare these data points to the extreme top of the theoretical peak for converged states. We will also find it convenient to display some data with histogram bars. Provided we choose the width of a rectangular bar to be 250 keV, we can compare the height of the bar to these "data points" and the area of the bar to the area under the Gaussian curve.

The eigenvectors for the observed states are formed at the end of the sequence of iterations so that we can calculate such things as the spectroscopic factor for proton stripping to these states and the $B(M1)$ transition rate between them. The spectroscopic factor defined by

$$C^2S_p = \langle\Psi_{6^-,T}(^{\text{A}}\text{Z})|| \ a^\dagger_{f_{7/2},\text{proton}} \ ||\Psi_{\frac{5}{2}^+}(^{\text{A}-1}\text{Z} - 1)\rangle^2 \tag{10}$$

(reduced in spin space only) is calculated directly from the respective wave functions, where we form the $A - 1$ ground state following the same procedure that we used for the mass-A ground state. (Note that the square of the

isospin Clebsch-Gordan coefficient is $C^2 = \frac{1}{2}$ for the cases considered here.) The $B(M1)$ rate for electromagnetic decay of the 6^-, $T = 1$ state to the yrast 6^-, $T = 0$ state is evaluated by using the appropriate $J = 1$ spectroscopic amplitudes [defined similarly to those given in Eq. (2)] in ALLWRLD [44].

Following AL, we do not do anything about the presence of spurious center-of-mass motion in our wave functions. There is no practical way to separate spurious motion in anything less than a full $1\hbar\omega$ calculation. We do measure the spuriosity of the states of interest by evaluating the diagonal matrix element of the center-of-mass Hamiltonian. These results and their significance are discussed in Sec. IV, where it is clear that spurious components are of consequence for mass 20 and 24 only.

All calculations were done with the VLADIMIR system of codes [45] adapted to UNIX and optimized for the ETA^{10} and Cray Y-MP computers at Florida State.

III. RESULTS

We now discuss, in turn, our results for ^{28}Si (some of which were presented previously in Ref. [1]), ^{32}S (some of which were shown in Ref. [34]), ^{24}Mg, ^{20}Ne, and ^{36}Ar. For each case we summarize our main findings in a figure showing the spectrum of $T = 0$ and $T = 1$ $M6$ strength, constructed as described above in conjuction with Eq. (8) and Eq. (9), compared to existing experimental data. Tables give additional detail on states of particular interest.

A. ^{28}Si

The ^{28}Si case, since it is in the middle of the *sd* shell, requires the largest basis space of the nuclei studied here. There are 28 908 $T = 0$ and 53 637 $T = 1$ 6^- states in a basis of 420 814 Slater determinants for the $n_{\max} = 8$ case, which is to be compared to 321 876 Slater determinants for the $n_{\max} = 4$ case reported earlier [1] and 802 for the AL ($n_{\max} = 0$) case [29]. Although the large basis size makes calculations for ^{28}Si more difficult than the other cases considered, the additional degrees of freedom also make this case arguably the most interesting to study since deformation and collective behavior in the core should be handled better than in a smaller basis space; nonetheless, as we shall see later, this does not guarantee that all of the important degrees of freedom have been included in the calculation. It is also the case that the ^{28}Si stretched states have been studied extensively [2, 46–58], providing a diverse set of experiments to test our model wave functions.

Figure 1 and Table I show the results of our calculations after 24 Lanczos iterations for each isospin. The solid curve in Fig. 1 is the spectrum predicted by the $n_{\max} = 8$ work, while the dashed curve shows the $n_{\max} = 4$ result that was the subject of the preliminary study reported in our earlier paper [1]. The two curves are essentially the same, justifying the truncation used in that preliminary study. The curves in the figure compare well with the two sets of data shown in the figure. The "data points" represent strengths deduced from

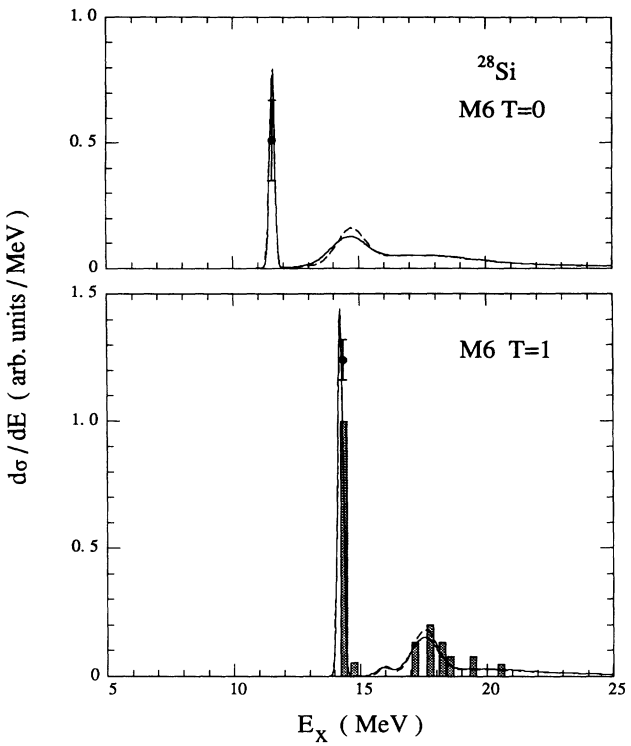

FIG. 1. Solid curves showing the predicted strength function for inelastic scattering to $T = 0$ (top) and $T = 1$ (bottom) 6^- states in ^{28}Si obtained with the $n_{\max} = 8$ basis are compared to "data points" (denoting the inelastic scattering results) and a histogram [denoting the (p, n) results] representative of the observed scattering strength. As discussed in the second half of Sec. II, the data points should be compared to the peak of the strength-function curve and the top of the histogram bar; the shaded area of the histogram also can be compared to the area under the strength-function curve. The dashed curve shows our earlier results [1] with the $n_{\max} = 4$ basis.

electron [46] and/or proton [49, 53–55] and pion [50] scattering and are displayed as described in the second half of Sec. II. (These points should be compared to the top of the peak in the theoretical spectrum.) The shaded histogram represents strengths deduced from the (p, n) reaction [47, 48], again displayed as described in Sec. II. (The height of the histogram bar can be compared to the data point and the shaded area of the bar can be compared to the area under the theoretical curve.) The excitation energies in ^{28}P have been shifted based on the 9.316 MeV excitation energy of the 3^+ $T = 1$ ground-state analog in ^{28}Si. The experimental strengths given in Table I are a composite of the two isovector strengths shown in the figure, with a larger error bar to accommodate the scatter in the measurements. (Remember that the energy of the yrast 6^- $T = 0$ state is in perfect agreement with experiment since it was used to fix the $f_{7/2}$ single-particle energy.) One notes quite good agreement for the energy gap between the $T = 0$ and $T = 1$ states and for their respective strengths.

We can summarize the theoretical results for both isospins as follows: almost $\frac{1}{4}$ of the strength is lost because of depletion of the $d_{5/2}$ orbit ($\Sigma = 0.77$ instead of 1) in the ground state; from $\frac{1}{4}$ to $\frac{1}{2}$ of the remaining strength is in the yrast state, which is the strongest state in the spectrum; about $\frac{1}{4}$ is in a cluster about 3–4 MeV above the yrast state; and the remainder is scattered thinly over the next 30–40 MeV. Configuration mixing leads to a single yrast state with a small fraction of the total strength while the bulk of the ESPHM strength is difficult to observe. (The figure in Ref. [1] contrasted the spectra predicted by AL with the $n_{\max} = 4$ curve shown here, emphasizing the fact that the extra $T = 0$ strength predicted by AL to lie below the $T = 1$ states, which should be seen experimentally but is not, is essentially eliminated now.) The fragmentation effects are greater for the $T = 0$ states, explaining their relatively greater reduction in strength. This is the key result, emphasized in Ref. [7], that cannot be obtained in core polarization models with realistic forces [22, 18]. We will discuss the bump region above the yrast state more extensively at the end of this section.

Table I provides a summary of the $M6$ transition rate and other predicted properties of the lowest 6^- states and compares them with the measured values [46–59]. Results from the simple model (ESPHM) and the AL calculation [29] are included to illustrate the apparent slow convergence of the calculations toward experiment as the basis size increases. Notice that the results for the isovector state are very good, and one anticipates that core polarization corrections such as those made in Ref. [23] could easily remove the remaining small discrepancies. In contrast, the isoscalar state seems to require some additional mixing to push more strength to higher excitation energies. It should be noted, however, that if we reconstruct Table I to include all observable low-lying strength, as we did in Ref. [61], it is clear that a steady improvement is being made.

1. Examination of effects from the core

Although the results above clearly indicate a problem with the $T = 0$ spectrum in ^{28}Si, they do not shed much light on the precise reason for the slower convergence of the $T = 0$ calculation. Another approach to the analysis of our results, proposed in a Comment by Geesaman and Zeidman [62] on our original paper, does provide some in-

TABLE I. Measured properties of the lowest observed $T = 0$ and $T = 1$ 6^- states in ^{28}Si compared to results from the simple model ($f_{7/2}d^{11}_{5/2}$), the AL model ($n_{\max} = 0$) from Ref. [29], $n_{\max} = 4$ results from our earlier paper [1], and the full space ($n_{\max} = 8$) results of this work. The energies of these states are from the compilation of Ref. [59].

Observable	Simple	$n_{\max} = 0$	$n_{\max} = 4$	$n_{\max} = 8$	Experiment
"Sum rule" Σ	1.0	0.854	0.785	0.771	
$E_x(T = 0)$ (MeV)		11.58	11.58	11.58	11.576
Z^2	1.0	0.258	0.203	0.198	0.13 ± 0.04[a]
C^2S_p	0.5	0.206	0.156	0.154	0.22 ± 0.04[b]
$R_0 = Z_0^2/S_p^0$	1.0	0.63	0.65	0.64	0.27 ± 0.10
$E_x(T = 1)$ (MeV)		13.02	14.23	14.23	14.357 ± 0.002
Z^2	1.0	0.522	0.374	0.369	0.29 ± 0.04[c]
C^2S_p	0.5	0.368	0.234	0.228	0.20 ± 0.02[b]
$R_1 = Z_1^2/S_p^1$	1.0	0.71	0.80	0.81	0.73 ± 0.12
$R = R_0/R_1$	1.0	0.88	0.81	0.80	0.37 ± 0.15
$T = 1 \rightarrow T = 0$ transition					
$B(M1)$ (e^2 fm^2)	0.162	0.073	0.052	0.053	0.031 ± 0.004[d]
ΔE (MeV)	0.70	1.44	2.65	2.65	2.78
Basis size (6^-, $T = 0$)	1	95	21 653	28 908	
Basis size (6^-, $T = 1$)	1	144	40 386	53 637	

[a] Average of values obtained from the data in Refs. [49], [50], and [53–55] by the analyses of Refs. [6–8,11], and [60] with appropriate error estimate; value is relative to $T = 1$ value from electron scattering.

[b] Average of results from Refs. [56] and [57] with appropriate error estimate; values differ slightly from those quoted in our previous paper [1] to correct errors in rounding.

[c] Average of values obtained from the data in Refs. [46–48] and the analyses of Refs. [5–12] with appropriate error estimate; value given is intermediate to the electron scattering result of 0.31 ± 0.01 and the (p, n) result of 0.25 ± 0.04. This average value, which is smaller than that quoted in our earlier paper [1], is more reasonable because of possible meson-exchange effects [12] not included in the (e, e') analyses.

[d] Reference [58].

sight. As Geesaman and Zeidman reminded us, the ratio of inelastic scattering strength [the square of Z defined in Eq. (2)] to single-particle transfer strength [the S defined in Eq. (10)] is a measure of the interference between the different fragments of the $d_{5/2}$ strength in the 6^- wave function. (This observation was first made in Ref. [63].) This ratio provides a useful method for examining issues related to core polarization and fragmentation.

We can see the relationship between the scattering and transfer strengths most clearly if we rewrite Eq. (2) as

$$Z_T^2 = \left| \sum_i \langle \Psi_{6^-,T} \| a^\dagger_{f_{7/2}} \| i \rangle \langle i \| a_{d_{5/2}} \| \Psi_{\text{g.s.}} \rangle \right|^2 , \qquad (11)$$

where $|i\rangle$ represents a $\frac{5}{2}^+$ state in the $A-1$ nucleus. The right-hand factor is then the proton-pickup strength going from ^{28}Si to ^{27}Al (for example) and the left-hand factor is the proton-stripping strength going from ^{27}Al to a particular 6^- state in ^{28}Si (the S_p in Table I). Hence, the ratio $R_T = Z_T^2/S_p^T$ for a state of isospin T is unity if the relevant $d_{5/2}^{-1}$ configuration in the 6^- wave function is concentrated in a single $\frac{5}{2}^+$ state. Deviations from unity reflect the interference between different ways of making the 6^- state that result from configuration mixing driven by the residual interaction. These ratios, and the double ratio $R = R_0/R_1$, are given in Table I.

[Note that the Comment discussed but never presented the ratio R_T, preferring to employ ratios Z_0^2/Z_1^2 and S_p^0/S_p^1 that help cancel systematic errors in the data. These ratios do not tell us anything until we form the double ratio R, thus hiding information that is specific to a particular isospin. In addition, systematic errors related to the treatment of the unbound nature of the $T=1$ state, when reducing the data to Z and S factors, are still present because of the large (up to 40%) corrections required. We prefer to rely on a comparison to data from a number of sources where some of the systematic errors are accounted for in the uncertainties from forming the average.]

Two things are immediately evident from the trends in R_T and a comparison to the data. One is that the ratios do not change much as we increase the basis size. This slow variation, particularly in R, is the signature of "fragmentation" and is to be expected. (There would be no change in R if we were in a pure weak-coupling regime.) The other observation is that R_1 is in agreement with the data. Deficiencies in the double ratio R are, again, due to shortcomings in the isoscalar results. It is important, however, that the gradual improvement in R with increasing basis size is due to R_1 getting larger rather than R_0 getting smaller as is required. A more detailed examination of Eq. (11) will illustrate where the problem lies.

We have the ability to determine the individual single-particle matrix elements that contribute to the sum in Eq. (11). The relevant matrix elements, their products, and the sequence of partial sums for the series giving Z are shown in Table II. The dominance of the first term, which provides from 86% to 97% of the total, explains the slow variation in R. Notice that three terms suffice to get within 5% of the total, and that the relative phases of the respective terms in the $T=0$ and $T=1$ series are the same until that (relatively small) third term. It is this interference that causes R_0 (R_1) to become smaller (larger) than the value of 0.72 that would result from using only the first two terms in the series. Differences between the two isospin states arise entirely from the $f_{7/2}$ matrix element with the hole state, so further investigation should emphasize the sd-fp Hamiltonian and the role of the $f_{5/2}$ spin-orbit partner.

We also have examined the internal structure of these wave functions using a graphical tool that explicitly displays the occupancy of the single-particle orbits, allowing us to deduce the relative importance of various core-state spins in a weak-coupling picture of the 6^- states. These pictures (not shown) suggest that a small family of relatively low-spin ($\frac{5}{2}$, $\frac{7}{2}$, $\frac{9}{2}$, $\frac{11}{2}$) core states suffice to span the important degrees of freedom in the calculation. It might be useful to perform a diagonalization in such a weak-coupling picture rather than perform the full calculation.

2. *Bump region*

The preceding discussion has covered issues concerning $M6$ strength in ^{28}Si that were considered in our earlier

TABLE II. Individual contributions to the series in Eq. (11) for the lowest 6^- state of each isospin in ^{28}Si.

		$T=0$		$T=1$	
State i	$\langle i \| a_{d_{5/2}} \| \Psi_{\text{g.s.}} \rangle$	Term[a]	Partial sum	Term[a]	Partial sum
1	0.7761	0.4309	0.431	0.5242	0.524
2	−0.2443	0.0415	0.472	0.0476	0.572
3	0.2033	−0.0267	0.446	0.0138	0.586
4	0.0390	−0.0025	0.443	−0.0002	0.585
5	0.1371	−0.0033	0.440	0.0108	0.596
Total[b]			0.445		0.607

[a]We use "Term" to denote the product $\langle \Psi_{6^-,T} \| a^\dagger_{f_{7/2}} \| i \rangle \langle i \| a_{d_{5/2}} \| \Psi_{\text{g.s.}} \rangle$.

[b]The "Total" value is the $|Z|$ from Eq. (2), that is, the positive root of the sum of the full (infinite) series on the right-hand side of Eq. (11).

paper and other papers on the subject of stretched-state structure. There is, however, an important point that was overlooked in previous discussions of our results. We emphasized [1] the fact that our calculations eliminated the low-lying, relatively strong, easily observed $T = 0$ states evident in the AL spectrum. We failed to comment on the concentration of $M6$ strength about 3 MeV above the yrast state because we did not think it could be observed. Examination of the (p, n) spectrum in Fig. 1 of Ref. [64] shows a structure 3 MeV above the yrast $T = 1$ state that might suggest otherwise.

The data shown in Ref. [64] were subsequently analyzed and the strength in that bump appears to have an $L = 5$ angular distribution that would be consistent with a 6^- assignment [48]. There are indications that, for at least one state in this same region, electron-scattering data are consistent [65] with an $M6$ form factor that has a strength comparable to that measured in the (p, n) reaction. The bump in the (p, n) work contains about 0.17 ± 0.04 of the ESPHM strength, which should be compared to our result of 0.24 for the same region. This very good agreement can also be seen in Fig. 1, where it is clear that we get reasonably correct values for the centroid and width of this collection of fragmented strength.

The point we wish to make is that *where* the strength goes is an important test of the mechanism that removes it from the narrow, yrast state that has received most of our attention in the past. Although there are great difficulties in making such measurements, such studies are valuable. The biggest challenge will be in tracking the isoscalar strength, which easily can be lost in the background at high excitation.

Clearly a large basis with configuration mixing is an essential element in any detailed explanation of the spectral distribution of $M6$ strength in ^{28}Si. Diminishing returns from the effort to expand the basis are also evident. In particular, truncations that do not significantly alter the level occupancies of the ground state, such as that used in Ref. [1], gave essentially the same results as the full *sd*-shell calculation. Remaining disagreement between theory and data is limited mainly to the isoscalar strength distribution, which must require the inclusion of more complicated correlations in the core that would decouple Z from S_p for $T = 0$ states only.

B. ^{32}S

The space for the ^{32}S calculations is also quite large, with 16 392 $T = 0$ and 29 840 $T = 1$ 6^- states in a basis of 221 418 Slater determinants for the $n_{\max} = 8$ case, although only a third as many states are needed for the $n_{\max} = 4$ case. (Comparison with the AL basis is meaningless, since it is the same as the ESPHM result.) The $n_{\max} = 4$ calculations described here were reported in conjunction with a paper [34] presenting new (e, e') data for ^{32}S. The only other data for $M6$ excitations in mass 32 are from a (p, n) experiment [48] that had been reported in preliminary form at a conference [64] and was included in the analysis of Ref. [34]. There are no published data concerning the $T = 0$ spectrum, although pion scattering experiments have been performed [66] that would provide such information.

Figure 2 and Table III show the results of our calculations after 56 Lanczos iterations for each isospin. The additional iterations were required in this case so that we could obtain converged (narrow) states for the addtional observable fragments seen in this nucleus. As before, the solid curve in the figure displays the $n_{\max} = 8$ spectrum and the dashed curve shows the $n_{\max} = 4$ result. However, since the $f_{7/2}$ single-particle energy was fixed by the ^{28}Si calculation described above, the theoretical excitation energies are now parameter-free predictions. The "data points" represent strengths deduced from electron scattering [34], while the shaded histogram represents strengths deduced from the (p, n) reaction [48], both constructed as described in the second half of Sec. II. The excitation energies in ^{32}Cl from the (p, n) measurement have been shifted based on the 7.002 MeV excitation energy of the 1^+ $T = 1$ ground-state analog in ^{32}S. Some of the data are also given separately in Table III.

There are significant qualitative differences between the spectra shown in Fig. 2 and the spectra for ^{28}Si shown in Fig. 1. Both theory and experiment have the new feature that the lowest 6^- $T = 1$ state is not the strongest state. Further, the number of observable fragments has increased for both $T = 0$ and $T = 1$ transitions, although

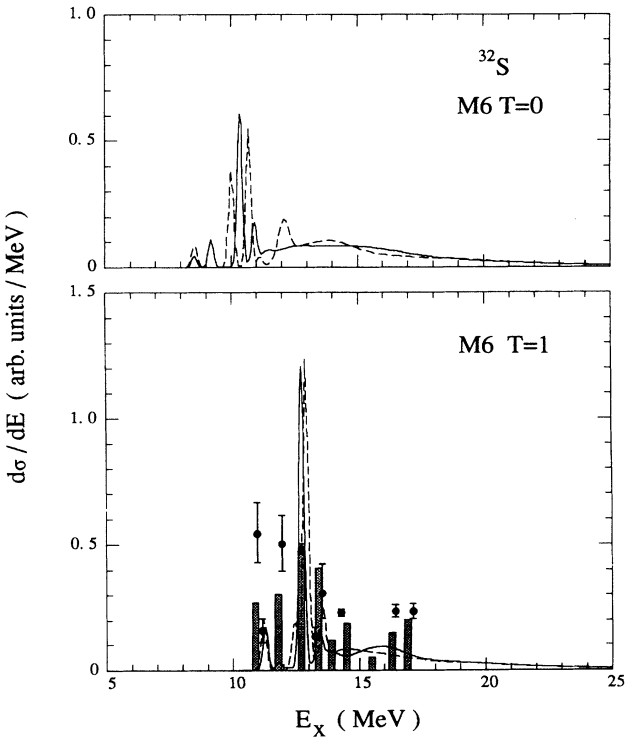

FIG. 2. Solid curves showing the predicted strength function for inelastic scattering to $T = 0$ (top) and $T = 1$ (bottom) 6^- states in ^{32}S obtained with the $n_{\max} = 8$ basis are compared to "data points" [denoting (e, e') results] and a histogram [denoting (p, n) results] representative of the observed scattering strength. The dashed curve shows our earlier results [34] with the $n_{\max} = 4$ basis.

TABLE III. The predicted locations and strengths of the first few $M6$ transitions in ^{32}S are given in the first four columns, with results for the truncated basis given first. The energies are in MeV. The $n_{max} = 4$ basis gives a total of 5545 $T = 0$ and 10 002 $T = 1$ states and $\Sigma = 0.936$. The full $n_{max} = 8$ basis gives a total of 16 392 $T = 0$ and 29 840 $T = 1$ states and $\Sigma = 0.903$. The data for the $T = 1$ strength from Refs. [34] and [48] are presented so that corresponding states are listed on the same line. We assume a Coulomb shift of about 7.0025 MeV for the ^{32}Cl data based on the location of the analog of the ^{32}Cl ground state in ^{32}S. Uncertainties in the data are about 0.1 MeV in excitation energy and about 10% in strength for the (e,e') data and about 20% in strength for the (p,n) data.

$n_{max} = 4$		$n_{max} = 8$					
$E_{th}(^{32}S)$	Z_0^2	$E_{th}(^{32}S)$	Z_0^2				
8.55	0.023	8.54	0.011				
10.02	0.098	9.20	0.028				
10.71	0.138	10.36	0.152				
$n_{max} = 4$		$n_{max} = 8$		(e,e') data[a]		(p,n) data[b]	
$E_{th}(^{32}S)$	Z_1^2	$E_{th}(^{32}S)$	Z_1^2	$E_x(^{32}S)$	Z_1^2	$E_x(^{32}Cl)$	Z_1^2
11.23	0.055	11.24	0.042	10.98	0.135	3.8	0.068
...		...		11.17	0.030	...	...
12.45	0.051	11.84	0.007	11.94	0.126	4.7	0.077
12.91	0.306	12.74	0.302	12.74	0.121	5.6	0.119
...		...		13.26	0.036	...	...
13.57	0.053	13.42	0.033	13.54	0.087	6.3	0.102

[a] Reference [34].
[b] Reference [48].

details concerning the number and location of these fragments varies with the basis truncation. The most obvious difference is that the number of $T = 0$ peaks is reduced in the larger space, much as we saw for ^{28}Si. The change is large enough to make the table in Ref. [34] obsolete, since that work only included the $n_{max} = 4$ results.

Although theory places too much strength in a single state near the centroid of the experimental isovector strength, it is clear that the experimental distribution has similar low-order moments to that predicted by our model. This appears to support our contention that fragmentation is responsible for the redistribution of stretched strength, even though we do not get the details precisely correct. To make this spectral comparison quantitative, we have evaluated the various moments over the region studied in these experiments. This is more accurate than a simple comparison to Σ since there is a fair amount of unobservable strength in the long tail above about 17 MeV excitation in ^{32}S. We get $\int = 0.77$ for the integral of the theoretical $T = 1$ spectrum over the ~ 7 MeV region where data were measured. This is reduced from $\Sigma = 0.90$ and compares very well to the electron-scattering total of 0.71 ± 0.05 [34], although it does exceed the result of 0.55 ± 0.09 from the charge-exchange experiment [48] by a substantial amount. The centroid of this strength is predicted to occur at 13.6 MeV, and is seen at 13.1 MeV (electron scattering) and 13.3 MeV (charge exchange) in the experiments. The width is predicted to be 1.5 MeV, and is observed to be about 2.0 MeV (electron scattering) and 1.8 MeV (charge exchange) in the experiments. This is quite good agreement.

Examination of Fig. 2 and the various integral moments shows that there is a significant disagreement between the (e,e') and (p,n) experiments on some details of the strength distribution. (Recall that the height of a histogram bar would be the same as a data point if the measured scattering strengths were the same.) The states at and above 12.7 MeV are perfectly consistent given the differences in experimental resolution, the possible size of meson-exchange corrections [12], and the reliance on distorted-wave approximation calculations for extraction of the charge-exchange strengths. The level of agreement is similar to that seen in other cases. The difference between the two data sets is limited to the strength of the first two states, where the two experiments disagree by a factor of more than 2. Since we do notice the predicted presence of $T = 0$ states within an MeV of these states, it is possible that isospin mixing could be the source of these differences. The (p,n) experiment would be seeing the "true" (unmixed) isovector spectrum. Comparison of π^+ to π^- scattering would tell us if mixing is the source of this disagreement.

As one might expect [34], the additional information seen in the $M6$ spectrum is associated with some differences in how the $d_{5/2}$ strength is fragmented in the core. The structure of the ^{32}S ground state, where the $2s_{1/2}$ orbit has been filled, is noticeably different from that of the ^{28}Si ground state. Single-nucleon pickup reactions populate several $d_{5/2}$-hole states (with similar strength) in ^{31}P but only one in ^{27}Al [59]. The same pattern is seen in the ground-state wave functions calculated with the BHW Hamiltonian. The entry in the second column of Table IV, when squared, is proportional to the $d_{5/2}$ pickup strength. These values indicate that the pickup strength is more balanced between the first three $\frac{5}{2}^+$ states in ^{31}P

TABLE IV. Individual contributions to the series in Eq. (11) for the third excited 6^- state of each isospin in ^{32}S. For comparison, note that the series for the first $T = 0$ state only gets to 68% of the total after 5 terms with the first term of the series being three times bigger than the final answer, while the series for the first $T = 1$ state gets to 83% of the total after 5 terms but also starts out about twice as big as the final answer.

		$T = 0$		$T = 1$	
State i	$\langle i \| a_{d_{5/2}} \| \Psi_{g.s.} \rangle$	Term[a]	Partial sum	Term[a]	Partial sum
1	0.5762	0.2652	0.265	0.2620	0.262
2	0.3632	0.1045	0.370	0.1546	0.417
3	−0.3662	0.0654	0.435	0.1280	0.545
4	0.1668	−0.0123	0.423	−0.0175	0.527
5	0.2417	−0.0207	0.402	0.0138	0.541
Total[b]			0.390		0.549

[a] We use "Term" to denote the product $\langle \Psi_{6^-,T} \| a^\dagger_{f_{7/2}} \| i \rangle \langle i \| a_{d_{5/2}} \| \Psi_{g.s.} \rangle$.

[b] The "Total" value is the $|Z|$ from Eq. (2), that is, the positive root of the full sum of the (infinite) series on the right-hand side of Eq. (11).

than it was in ^{27}Al (cf. Table II), in rough agreement with experiment.

Table IV also shows the decomposition of Eq. (11) into the sequence of partial sums for the third 6^- states, which are the strongest $T = 0$ and $T = 1$ states in our calculations. It is clear that the fragmentation of the $M6$ strength is reflected in the convergence of the sequence of partial sums for the series giving Z. The first term is no longer dominant, providing only 48% of the total for the $T = 1$ state. Both series oscillate so that 5 terms are required before the series begins to settle down near the answer. This effect is most dramatic for the $T = 0$ case. The situation for the lowest states is much worse, with larger oscillations and much slower convergence. Thus, it is clear that increased fragmentation is associated with a breakdown in simple weak-coupling pictures of these states. It might be interesting to see the results of 3-particle transfer reactions for these states. Certainly the fragmentation of the $d_{5/2}$-hole strength has an important role in spreading the $M6$ strength as we approach the end of the shell. Model-space limitations on our description of this effect are discussed at the end of Sec. III D.

C. ^{24}Mg

The size of the basis for the ^{24}Mg calculations is relatively small, with 5111 $T = 0$ and 8919 $T = 1$ 6^- states in a basis of 58 902 Slater determinants for the $n_{\max} = 8$ case, which is marginally larger than the 57 764 Slater determinants for the $n_{\max} = 4$ case. There are 2116 Slater determinants in the AL basis ($n_{\max} = 0$) where there are only a few hundred states possible. (AL never did this particular calculation, although they did publish results for ^{26}Mg [63].) The experimental situation is fair for ^{24}Mg, consisting of early electron and proton scattering data on the $T = 1$ states [67,68,49] and recent results for the $T = 0$ state from pion scattering [69] and the $T = 1$ strength distribution from the (p, n) reaction [48].

Figure 3 and Table V show the results of our calculations after 30 Lanczos iterations (we did a few more in this case since they go quite fast) for each isospin. The solid curve in the figure is from the $n_{\max} = 8$ run while the dashed curve shows the result in the $n_{\max} = 4$ basis, both compared to "data points" representing the electron [68], proton [49], and pion [69] scattering results and to

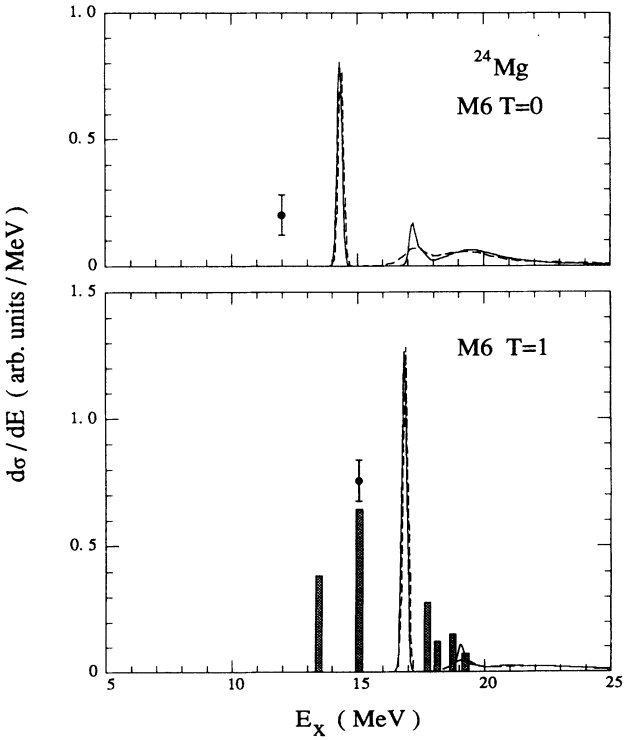

FIG. 3. Solid curves showing the predicted strength function for inelastic scattering to $T = 0$ (top) and $T = 1$ (bottom) 6^- states in ^{24}Mg obtained with the $n_{\max} = 8$ basis are compared to "data points" (denoting inelastic scattering results) and a histogram [denoting the (p, n) results] representative of the observed scattering strength. The dashed curve shows results with the $n_{\max} = 4$ basis.

TABLE V. Measured properties of the lowest observed $T = 0$ and $T = 1$ 6^- states in ^{24}Mg compared to results from the simple model ($f_{7/2}d^{11}_{5/2}$), our results within the AL model space ($n_{max} = 0$), and this work.

Observable	Simple	$n_{max} = 0$	$n_{max} = 4$	$n_{max} = 8$	Experiment
"Sum rule" Σ	0.667	0.576	0.501	0.498	
$E_x(T = 0)$ (MeV)		13.63	14.36	14.30	12.05 ± 0.10
Z^2	0.667	0.315	0.204	0.202	0.05 ± 0.02[a]
C^2S_p	0.5	0.326	0.271	0.271	...
$R_0 = Z_0^2/S_p^0$	0.67	0.48	0.38	0.37	...
$E_x(T = 1)$ (MeV)		15.49	16.90	16.83	15.135 ± 0.03[b]
Z^2	0.667	0.450	0.322	0.320	0.19 ± 0.02[c]
C^2S_p	0.5	0.404	0.344	0.344	...
$R_1 = Z_1^2/S_p^1$	0.67	0.56	0.47	0.46	...
$R = R_0/R_1$	1.0	0.87	0.80	0.80	...
$T = 1 \rightarrow T = 0$ transition					
$B(M1)$ (e^2 fm^2)	0.142	0.050	0.044	0.044	...
ΔE (MeV)	0.66	1.86	2.53	2.53	3.1 ± 0.2
Basis size (6^-, $T = 0$)	1	214	4963	5111	
Basis size (6^-, $T = 1$)	1	341	8686	8919	

[a]Value reported by Ref. [69] with an estimate of its uncertainty; a previous analysis, by Ref. [7] of data from Ref. [49], gave upper limit of 0.07 on the strength in a region around 11.3 MeV.

[b]The value in Ref. [59] is based partially on an excitation energy from Ref. [67] that was subsequently corrected [68] to 15.13 ± 0.04 MeV; our value is an average of this new value with that of Ref. [49].

[c]Average of values obtained from the data of Refs. [67] and [68] by the analyses of Refs. [5–7] and [9,10,12] with appropriate error estimate; may need reduction for meson-exchange effects.

a shaded histogram representing the results for isovector strength from a (p, n) measurement [48]. The data are plotted following the procedure described in Sec. II, and the excitation energies in ^{24}Al from the (p, n) measurement have been shifted based on the 9.515 MeV excitation energy of the 4^+ $T = 1$ ground-state analog in ^{24}Mg. The experimental entries in Table V are a composite of both data sets. The calculated energies given in Table V and Fig. 3 are predictions since the s.p.e. is fixed by the ^{28}Si results shown previously. The two curves in the figure are essentially identical because the spaces are nearly the same size; the differences are due mainly to the fact that we performed fewer iterations (24 instead of 30) for the smaller case in our initial runs.

In contrast to the ^{28}Si situation, there is a significant disagreement between theory and experiment for ^{24}Mg. We predict a single strong state that is not seen in the data. Our initial interpretation, prior to the availability of the (p, n) data, was to identify our peak with the $T = 1$ state seen in electron and proton scattering. It would then appear that we place the strength about 2 MeV above the data and that we overpredict the $M6$ strength by factors of 1.7 and 4 for the $T = 1$ and $T = 0$ transitions, respectively, as indicated in Table V. The result is an improvement over the AL basis but remains far from the data. The new (p, n) data suggest a very different interpretation [48]: that we predict the centroid for the $M6$ strength within about a MeV but that we do not have sufficient fragmentation of the strength about that centroid. If we examine the strength over the $13 \leq E_x \leq 20$ MeV region covered in the experiment, we predict an integrated strength of about $Z^2 = 0.37$ compared to the 0.41 ± 0.06 observed, and we predict a centroid of 17.1 MeV compared to the 15.9 MeV centroid of the observed strength. The strength is correct, but a stronger $H_{sd\text{-}fp}$ interaction seems required to pull the centroid down about 1 MeV. We will say more about this issue later.

The primary uncertainty with regard to the interpretation above is whether the (p, n) experiment is seeing $M6$ strength accurately despite the relatively poor resolution achievable in such experiments. The charge-exchange and electron-scattering experiments agree on the strength of the state near 15 MeV, so the method employed is consistent for strong states. [The (e, e') and (p, n) results for ^{28}Si (Fig. 1) and ^{32}S (Fig. 2) also agree quite well for most cases.] It is unfortunate that the electron-scattering work [68] does not include results for form factors of the complexes seen around 13–13.5 MeV and 18 MeV in the (e, e') spectrum, complexes that could plausibly be associated with the strength seen in (p, n). The proton scattering spectrum [49] and the pion scattering spectrum [69] do not show states at the particular energies expected from the (p, n) work, but there are peaks in the vicinity whose cross-section angular distributions are not shown. Isospin mixing could move the strength from the position expected based on simple analog arguments and would require careful analysis, and perhaps

TABLE VI. Individual contributions to the series in Eq. (11) for the lowest 6^- state of each isospin in ^{24}Mg.

		$T=0$		$T=1$	
State i	$\langle i\|\|a_{d_{5/2}}\|\|\Psi_{g.s.}\rangle$	Term[a]	Partial sum	Term[a]	Partial sum
1	0.6524	0.4805	0.480	0.5410	0.541
2	0.0323	0.0007	0.481	−0.0041	0.537
3	0.1991	−0.0300	0.451	0.0141	0.551
4	0.0795	−0.0003	0.451	0.0030	0.554
5	−0.0161	−0.0007	0.450	0.0005	0.555
Total[b]			0.449		0.566

[a]We use "Term" to denote the product $\langle\Psi_{6^-,T}\|a^\dagger_{f_{7/2}}\|i\rangle\langle i\|\|a_{d_{5/2}}\|\|\Psi_{g.s.}\rangle$.

[b]The "Total" value is the $|Z|$ from Eq. (2), that is, the positive root of the full sum of the (infinite) series on the right-hand side of Eq. (11).

new experiments, to decide if this low-lying strength is real.

Conclusions about the isoscalar spectrum are more difficult to reach. Such experiments are difficult because background problems are more severe than with reactions that select the isovector channel in isolation. There is only a single 6^-, $T=0$ state known [69], and it is very weak. Given that we presume our theoretical $T=0$ spectrum has the same defects as our $T=1$ spectrum, it seems likely that many unseen fragments of $T=0$ strength are distributed between 12 and 16 MeV. Finding these fragments would be very helpful, but will pose a challenge experimentally.

Table V summarizes what we know about the main states in the spectrum and how the predictions depend upon basis truncation. As is also clear from Fig. 3, the tiny increase in basis size from $n_{\max}=4$ to $n_{\max}=8$ has negligible effects on the spectrum, but there is a marked improvement from what AL would have obtained in the $n_{\max}=0$ basis truncation. There is also a systematic decrease in both R_0 and R_1, with a marginal decrease in the ratio of ratios R. (Unfortunately, there are no transfer reaction data for this nucleus that would provide the proton stripping value we require.) Notice that the value for R is essentially identical to that in ^{28}Si (cf. Table I). Inspection of Table VI, which shows the convergence of the series defined in Eq. (11), makes it evident that this occurs because the states in ^{24}Mg are driven by a dominant core configuration just as was the case in ^{28}Si; however, the data tell us that this picture is wrong for ^{24}Mg. Assuming that the core structure from the BHW Hamiltonian is reasonably correct, we should investigate the role of $1p\rightarrow sd$ excitations (and perhaps the role of the $f_{5/2}$ orbit) on fragmentation of these states.

We now return to the question of the validity of the $H_{sd\text{-}fp}$ from ST that we employed in our calculations (cf. Sec. II). Our calculations did not introduce any A dependence for the strength of this part of the Hamiltonian (while we did include the slow $A^{-0.3}$ dependence of the BHW H_{sd}) because our original goal was to leave this part of the AL interaction fixed. Further, it is difficult to obtain guidance from electron-scattering fits because of their scatter: fits for ^{28}Si and ^{32}S have ranged over $1.63\leq b\leq 1.80$ [46, 34], reflecting the difficulty fitting the radial form of these unbound states. The ST interaction was evaluated with $b=1.847$, corresponding to the value predicted by $\hbar\omega\approx 41.4/A^{1/3}$ for $A=40$, which is reasonable for these states in Si and S. We would expect b to get larger for smaller A, thereby strengthening the sd-fp Hamiltonian as is clearly required here.

We made some test runs to verify the sensitivity of our results to the strength of the coupling between the shells. A search between $b=1.65$ and $b=1.85$ quickly verified that use of $b=1.745$ (a standard $A\approx 28$ value) gives a centroid at 15.9 MeV with a strength of $Z_1^2=0.387$ when integrated over the same 13 MeV $\leq E_x\leq$ 20 MeV region where we have experimental data. Qualitatively the isovector spectrum is not changed, with a strong peak containing $Z^2=0.306$ at 15.3 MeV. Hence it is clear that a plausible increase in the strength of H_{sd-fp} is enough to fix the ≈ 1 MeV error in the centroid location but will not change the fragmentation of the spectrum. There are somewhat larger effects on the isoscalar spectrum, with more fragmentation accompanying the lower energy for the centroid, but there are no data we can use to evaluate the significance of this change.

D. ^{20}Ne and ^{36}Ar

For completeness, we also present results for the other two $N=Z$ sd-shell nuclei. The number of degrees of freedom is quite small (similar in magnitude to the size of the AL space for mid-shell nuclei) so close to the closed-shell nuclei, hence they should be interpreted with caution; they mainly serve to illustrate the limitations of our model-space truncation. There are only 318 Slater determinants (57 $T=0$ and 79 $T=1$ 6^- states) for ^{20}Ne and 7178 Slater determinants (816 $T=0$ and 1315 $T=1$ 6^- states) for ^{36}Ar. Only the full-space calculations were done since other truncations make no sense for these nuclei.

Figure 4 and Table VII show the results of our calculation for the ^{20}Ne nucleus after 20 iterations. Our model places essentially all $M6$ strength in a single peak, which is at variance with the charge-exchange data [48] shown with the shaded histogram. This histogram was constructed by the procedure described in Sec. II, and the excitation energies in ^{20}Na have been shifted based

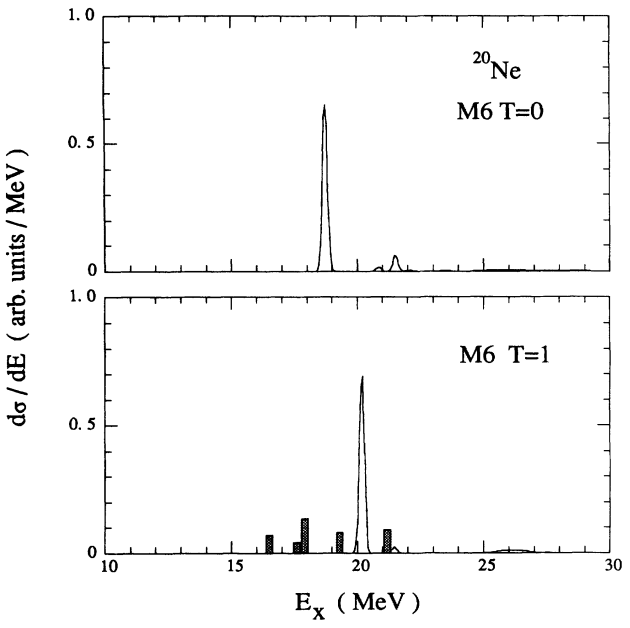

FIG. 4. Solid curves showing the predicted strength function for inelastic scattering to $T = 0$ (top) and $T = 1$ (bottom) 6^- states in ^{20}Ne obtained with the $n_{max} = 8$ basis are compared to a histogram representative of the scattering strength observed with the (p, n) reaction.

on the 10.274 MeV excitation energy of the 2^+ $T = 1$ ground-state analog in ^{20}Ne. (Data have been taken with the (p, p') reaction also [70], but no analysis has been published.) The situation is similar to the problem noted in the ^{24}Mg case (Fig. 3) above. The centroid of the (p, n) data is at about 18.5 MeV with a total strength of $Z^2 = 0.107 \pm 0.017$ compared to our total strength of 0.176 (essentially all of $\Sigma = 0.201$) located at 20.2 MeV. Clearly we require a stronger $H_{sd\text{-}fp}$ to lower the centroid by about 1.7 MeV—more than was required for ^{24}Mg, as might be expected. (If such a shift is required, and given our underestimate of the isovector fragmentation, we would expect the isoscalar strength will be distributed within a several-MeV-wide region centered around 17 MeV.) The amount of isovector $M6$ strength is consistent with our model prediction, but we have no explanation for the fragmentation that has been seen here and in ^{24}Mg.

The ^{20}Ne case, because of its small basis size, is a good candidate for exploring the effects of $1p \rightarrow sd$ excitations on the fragmentation of $M6$ strength in the lower part of the shell. Indeed, full $1\hbar\omega$ calculations should be feasible for ^{20}Ne, thereby allowing study of the importance of these excitations and also permitting the elimination of spurious motion problems that, as discussed in Sec. IV below, are significant for this nucleus. We have not pursued such calculations at this time because our focus has been on a schematic $f_{7/2} + sd$ model consistent with our principle emphasis on mass 28 and 32 nuclei, but they would certainly be of interest.

Figure 5 and Table VIII show our results for ^{36}Ar after 56 iterations of the Lanczos process. The additional iterations were required by the complexity of the spectrum at low excitation energy, as is evident from the figure. There are no data for $M6$ strength in this nucleus, but we add for future reference that excitation energies in ^{36}K from (p, n) data would need to be shifted based on the 6.611 MeV excitation energy of the 2^+ $T = 1$ ground-state analog in ^{36}Ar. It is immediately evident that our predictions for ^{36}Ar are qualitatively similar to those for ^{32}S, with a number of observable fragments of $M6$ strength. The fragmentation has continued to increase as we approach the end of the shell, with only a small fraction (about 18%) of the total isovector $M6$ strength $\Sigma = 0.956$ in states below 12 MeV. About 23% is in the complex of states predicted at 12.3 ± 0.2 MeV that give rise to the peak seen in Fig. 5. It would be interesting to measure this spectrum, although caution is urged: the strongest states here are bigger than some

TABLE VII. Predicted properties of the lowest $T = 0$ and $T = 1$ 6^- states in ^{20}Ne with the $n_{max} = 8$ model space compared to results from the simple model $(f_{7/2}d^{11}_{5/2})$ and the available data.

Observable	Simple	$n_{max} = 8$	Experiment
"Sum rule" Σ	0.333	0.201	
$E_x(T = 0)$ (MeV)		18.74	...
Z^2	0.333	0.164	
$E_x(T = 1)$ (MeV)		20.18	≈ 17.8
Z^2	0.333	0.176	0.034 ± 0.006[a]
$T = 1 \rightarrow T = 0$ transition			
$B(M1)$ (e^2 fm^2)	0.142	0.084	...
ΔE (MeV)	0.98	1.44	
Basis size (6^-, $T = 0$)	1	57	
Basis size (6^-, $T = 1$)	1	79	

[a]Value for strongest state from Ref. [48] with appropriate error estimate; there are weaker states at both higher and lower energy for a total Z^2 of 0.107.

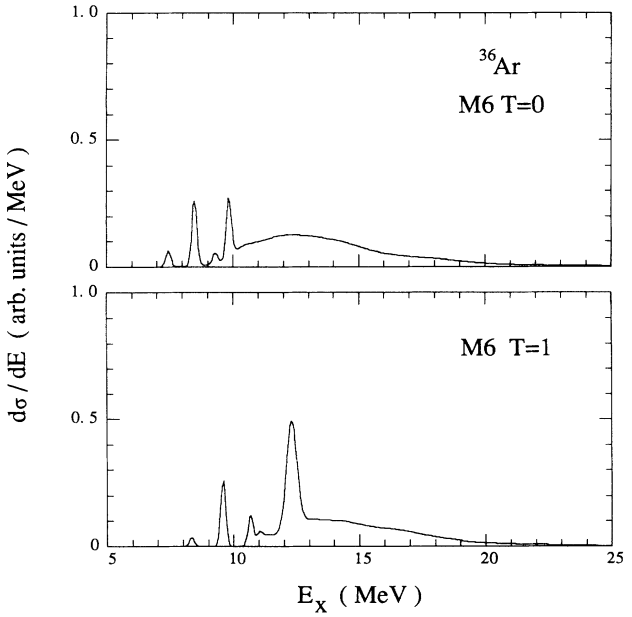

FIG. 5. The solid curves show the predicted strength function for inelastic scattering to $T = 0$ (top) and $T = 1$ (bottom) 6^- states in ^{36}Ar obtained with the $n_{max} = 8$ basis.

of those actually observed in ^{32}S, but the states may be weaker than predicted because it is likely that we have underestimated the fragmentation, as was the case for ^{32}S.

For perspective on this last statement, it is useful to look at what happens in ^{40}Ca. Our $n_{max} = 8$ model space corresponds to the simplest model for ^{40}Ca, giving $\Sigma = 1$ with all of the $T = 0$ strength in a single state at $E_x = 11.9$ MeV and all of the $T = 1$ strength in a single state at 12.6 MeV. A (p, n) experiment [71] sees 6^- $T = 1$ strength spread between 13 and 16.5 MeV with a centroid at about 14.7 MeV and a total strength of about $Z^2 = 0.42$. (Here we have converted the excitation energies in ^{40}Sc to ^{40}Ca based on the 7.7 MeV excitation energy in ^{40}Ca of the 4^- $T = 1$ analog to the ground state of ^{40}Sc. We have also converted the distorted-wave impulse approximation norm quoted to Z^2, but it should be noted that the t matrix used in Ref. [71] is not the same as the one used in Ref. [48].) Thus our prediction is lower in energy, as might be expected as we move to heavier nuclei without adjusting $H_{sd\text{-}fp}$, and fails to account for the observed spreading and reduction of $M6$ strength. The failure of a simple closed-shell model for ^{40}Ca is also evident in the fragmentation of $\frac{5}{2}^+$ states seen in single-nucleon pickup reactions [59]. We conclude that the *sd*-shell model space and BHW Hamiltonian cannot account for some important sources of $d_{5/2}$ spreading near the end of the shell, and thus our predictions for ^{36}Ar (and to a lesser extent, for ^{32}S) must underestimate the fragmentation of stretched $M6$ strength.

TABLE VIII. Predicted $M6$ strength for the lowest 6^- states in ^{36}Ar that were reasonably well converged. These are in the $n_{max} = 8$ basis space, where there are 816 $T = 0$ and 1315 $T = 1$ states and $\Sigma = 0.956$. Energies are in MeV, with the error indicating the width due to incomplete convergence of the calculation.

$T = 0$		$T = 1$	
E_{th}	Z^2	E_{th}	Z^2
5.52	10^{-5}	8.35	0.009
7.46	0.016	9.59	0.064
8.49	0.065	10.68	0.029
8.88±0.01	0.001	11.03±0.11	0.008
9.31±0.02	0.011	11.23±0.28	0.012
9.86±0.06	0.057	11.54±0.50	0.019

IV. DISCUSSION

Our particular emphasis in this paper has been on the new information that can be obtained by examining the *spectrum* of "stretched" strength in nuclei rather than focusing on just the size of the strongest state. It is important to remember what is special about these spin excitations: a one-step $M6$ transition from the 0^+ ground state to any 6^- state proceeds (within the limits of a $1\hbar\omega$ picture) through a unique configuration so that scattering experiments can be used to follow the fragmentation of this configuration among the many 6^- states. These transitions are interesting because they provide a means for looking at the spectrum of a particular configuration, i.e., the response to a single particle-hole creation operator rather than the response to more complicated operators that involve many particle-hole creation operators, such as $M1$ or $E2$ operators.

We have shown that the reduction and redistribution of $M6$ strength in $N = Z$ *sd*-shell nuclei can be described well by large-basis shell-model calculations; the loss of $M6$ strength results from fragmentation of the "stretched" configuration by conventional configuration mixing. The model gives a nearly quantitative description of the data for ^{28}Si and ^{32}S despite significant qualitative differences between the two spectra. In addition, the model shows greater fragmentation of $T = 0$ states than $T = 1$ states as is required by the data in ^{28}Si. We fail to describe the spectra for nuclei in the lower half of the *sd* shell (^{24}Mg and ^{20}Ne), but we do get the correct amount of low-lying observable strength. The results for the isovector response are summarized in Table IX. It appears that we need the full $1\hbar\omega$ space to get a correct description of the lighter nuclei.

The key ingredients in these calculations appear to be the use of a basis with sufficient degrees of freedom and an effective Hamiltonian that describes the correlations in the *sd* shell reasonably well. Both are important since it is the admixture of other 6^- configurations by mixing within the *sd* shell that has fragmented the "stretched" configuration. In the language of the projection-operator picture employed in Sec. I, it is the set of $|1\hbar\omega\rangle$ configurations that seems crucial to getting the spectral distribution of the $|M6\rangle$ configuration correct. Once this

TABLE IX. Summary of the isovector $M6$ strength predicted and observed in the $N = Z$ sd-shell nuclei. Here Σ is the "sum rule" defined in Eq. (5) while $\int$theory ($\int$data) is the sum of predicted (observed) strength over the approximate 6–8 MeV region of excitation energy where $M6$ strength has been extracted from the experimental data.

Nucleus	Σ	$\int$ theory	$\int$ data	Ref.
^{20}Ne	0.201	0.18	0.11 ± 0.02	[48]
^{24}Mg	0.498	0.37	0.41 ± 0.06	[48]
^{28}Si	0.771	0.70	0.43 ± 0.07	[48]
^{32}S	0.903	0.77	0.63 ± 0.08	[34, 48]
^{36}Ar	0.956	0.80	...	
^{40}Ca	1.000	1.00	0.42 ± 0.06	[71]

spectrum is satisfactorily established from a nonperturbative calculation, the effect of the $|C\rangle$ space on the strength distribution can be handled perturbatively as core-polarization modifications to the transition operator. The $|C\rangle$ configurations would act to fine tune the strength distribution once diminishing returns from enlarging the basis space are encountered—which would seem to be once the dominant effects of the $|1\hbar\omega\rangle$ space have been included.

This work raises a number of issues that need to be addressed experimentally. The present situation is that the $T = 1$ $M6$ response has been characterized by fairly complete (p, n) measurements that are calibrated by (e, e') data, but that very little is known about the $T = 0$ response. Knowledge of the $T = 0$ strength distribution from high-resolution (p, p') and (π,π') measurements would provide a crucial test of these model predictions. It is also unfortunately the case that the analysis of the older (e, e') data on ^{24}Mg and ^{28}Si did not report the form factors for peaks other than the isolated $T = 1$ 6^- states known to be interesting at the time. Repeating or reanalyzing these experiments would provide a valuable check on the isovector strengths extracted from the (p, n) data. Pion scattering data would be most helpful if it turns out that there is isospin mixing in ^{32}S, or to prove that there is no mixing in the nuclei considered here.

There are also a number of unresolved theoretical issues. Although we describe the ^{28}Si $T = 1$ spectrum very well, we do not get quite enough isovector strength in the lowest states in ^{32}S and we badly underestimate the fragmentation for ^{24}Mg and ^{20}Ne. The remainder of the full $1\hbar\omega$ basis, particularly that of the $f_{5/2}$ spin-orbit partner, may be important in this regard. It would certainly be interesting to see if the $f_{5/2}$ orbit would help with the $M1$ transition rate between the $T = 1$ and $T = 0$ states in ^{28}Si; unfortunately, this is a very large calculation. The rather crude choice for the Hamiltonian connecting the sd and fp spaces would need to be replaced if such work is pursued.

Another limitation on our calculations is that there is no practical way to separate spurious states and intrinsic states without doing a full $1\hbar\omega$ calculation. We can, however, evaluate the magnitude of the spurious center-of-mass motion in our wave functions as a measure of the errors introduced by our truncation. It turns out that this is not a serious problem for the mass-28 and -32 nuclei that are of primary interest to us. The measured spuriosity is small, typically less than 1% and decreasing with increasing A, for the states examined in mass $A \geq 28$ nuclei. The situation is worse in the lighter nuclei, with as much as 9% spuriosity in the strong $T = 0$ 6^- state in ^{24}Mg and more than 12% spuriosity in the $T = 1$ 6^- state in ^{20}Ne. The results for these nuclei cannot be trusted completely until full $1\hbar\omega$ calculations are done to permit the separation of center-of-mass and intrinsic states. As noted above, a larger model space for $A \leq 24$ calculations is suggested by other arguments also.

The full model interaction may need to be examined more closely also. Some of our failures are certainly an indication of the need for additional mixing, perhaps from different core deformation effects or mixing with configurations in the fp shell. The difficulty is that effects due to collective correlations in nuclei are not treated very efficiently in the shell model. Some are surely incorporated into $H_{\rm eff}$, but the corresponding change in the effective $M6$ operator has not been calculated. Core polarization and weak mixing calculations can help to clarify further the physics of stretched strength fragmentation. Also note that Schmid's work [72] for the positive parity states in ^{28}Si, with much larger model spaces and a different interaction in the sd shell, gives $\Sigma \cong 0.57$ which could eliminate much of the remaining discrepancy between theory and experiment for the $T = 1$ states. However, this result seems at variance with the $d_{5/2}$ occupation probability [73], which supports a $\Sigma \approx 0.75$ close to that obtained with the BHW Hamiltonian.

Finally, it is important to add that the experimentally observed states are slightly unbound, and the resulting change in the wave functions would affect both the $M6$ strength extracted from experiment [74] and the matrix elements that enter our Hamiltonian. Proper inclusion of continuum effects is an important open problem that is beyond the scope of this work, but there are methods [75] that can be used to address this problem [43].

In sum, fragmentation of the "stretched" state via conventional configuration mixing provides, within the limitations of our model space, a clear explanation of many observed properties of 6^- states seen in inelastic scattering from sd-shell nuclei. Effects due to our choice of interaction and basis truncation need to be explored to see if the remaining discrepancies can be understood. We emphasize that it is the full spectrum of the $M6$ response that provides the most stringent test of any model. The remaining experimental challenge is to devise means of using spin observables to map out the full strength distribution, even when it is otherwise obscured by background states.

ACKNOWLEDGMENTS

Special thanks are due to Rob Hausman for providing a copy of VLADIMIR and assisting in the initial conversion to the Cyber-205, to Bryon Anderson, Dick Lindgren,

and Stan Yen for allowing us timely access to their data, and to John Millener, Alex Brown, and Andy Bacher for some informative discussions. This work was supported in part by the Florida State University Supercomputer Computations Research Institute which is partially funded by the U.S. Department of Energy through Contract No. DE-FC05-85ER250000, and by LLNL through Contract No. W-7405-ENG-48.

[1] J.A. Carr, S.D. Bloom, F. Petrovich, and R.J. Philpott, Phys. Rev. Lett. **62**, 2249 (1989); **63**, 918(E) (1989).
[2] T.W. Donnelly, Jr., J.D. Walecka, G.E. Walker, and I. Sick, Phys. Lett. **32B**, 545 (1970).
[3] T.W. Donnelly and G.E. Walker, Ann. Phys. (N.Y.) **60**, 209 (1970).
[4] P.J. Moffa and G.E. Walker, Nucl. Phys. **A222**, 140 (1974).
[5] R.A. Lindgren, W.J. Gerace, A.D. Bacher, W.G. Love, and F. Petrovich, Phys. Rev. Lett. **42**, 1524 (1979).
[6] F. Petrovich, in *The (p,n) Reaction and the Nucleon-Nucleon Force*, edited by C.D. Goodman *et al.* (Plenum, New York, 1980), p. 115.
[7] F. Petrovich, W.G. Love, A. Picklesimer, G.E. Walker, and E. Siciliano, Phys. Lett. **95B**, 166 (1980).
[8] F. Petrovich and W.G. Love, Nucl. Phys. **A354**, 499c (1981).
[9] R.A. Lindgren and F. Petrovich, in *Spin Excitations in Nuclei*, edited by F. Petrovich *et al.* (Plenum, New York, 1984), p. 323.
[10] R.A. Lindgren, J. Phys. (Paris) Colloq. **C4-1984** (supplement to volume **45**), 433 (1984).
[11] F. Petrovich, J.A. Carr, and H. McManus, Annu. Rev. Nucl. Part. Sci. **36**, 29 (1986).
[12] R.A. Lindgren *et al.*, Can. J. Phys. **65**, 666 (1987).
[13] F. Petrovich, J.A. Carr, R.J. Philpott, and A.W. Carpenter, Phys. Lett. B **207**, 1 (1988).
[14] T. Suzuki, S. Krewald, and J. Speth, Phys. Lett. **107B**, 9 (1981).
[15] F. Osterfeld, S. Krewald, J. Speth, and T. Suzuki, Phys. Rev. Lett. **49**, 11 (1982).
[16] P. Blunden, B. Castel, and H. Toki, Nucl. Phys. **A440**, 647 (1985).
[17] G.E. Walker, Phys. Rev. C **5**, 1540 (1972).
[18] D.J. Rowe and S.S.M. Wong, Nucl. Phys. **A153**, 561 (1970); D.J. Rowe, S.S.M. Wong, H. Chow, and J.B. McGrory, *ibid.* **A298**, 31 (1978).
[19] S. Krewald and J. Speth, Phys. Rev. Lett. **45**, 417 (1980).
[20] I. Hamamoto, J. Lichtenstadt, and G. F. Bertsch, Phys. Lett. **93B**, 213 (1980).
[21] J. Speth, V. Klemt, J. Wambach, and G.E. Brown, Nucl. Phys. **A343**, 382 (1980).
[22] P. Blunden, B. Castel, and H. Toki, Z. Phys. A **312**, 247 (1983).
[23] A. Yokoyama and H. Horie, Phys. Rev. C **36**, 1657 (1987).
[24] K. Muto, Phys. Lett. B **213**, 115 (1988).
[25] L. Zamick, Phys. Rev. C **29**, 667 (1984).
[26] H. Liu and L. Zamick, Phys. Rev. C **32**, 1754 (1985).
[27] N.G. Goncharova and B.B. Matveev, Yad. Fiz. **42**, 99 (1985) [Sov. J. Nucl. Phys. **42**, 61 (1985)].
[28] D.J. Millener and D. Kurath, Nucl. Phys. **A255**, 315 (1975).
[29] A. Amusa and R.D. Lawson, Phys. Rev. Lett. **51**, 103 (1983).
[30] A.G.M. van Hees and P.W.M. Glaudemans, Z. Phys. A **314**, 323 (1983); **315**, 223 (1984).
[31] R.S. Hicks *et al.*, Phys. Rev. C **30**, 1 (1984).
[32] C.L. Morris *et al.*, Phys. Lett. **86B**, 31 (1979).
[33] C.F. Moore *et al.*, Phys. Lett. **80B**, 38 (1978).
[34] B.L. Clausen *et al.*, Phys. Rev. Lett. **65**, 547 (1990).
[35] Some portions of the full-space results for isovector $M6$ transitions were presented in the contribution by J.A. Carr, in *Spin and Isospin in Nuclear Interactions*, edited by S.W. Wissink, C.D. Goodman, and G.E. Walker (Plenum, New York, 1991), p. 333.
[36] B.H. Wildenthal, Prog. Part. Nucl. Phys. **11**, 5 (1984).
[37] J.P. Schiffer and W.W. True, Rev. Mod. Phys. **48**, 191 (1976).
[38] B.H. Wildenthal, J.B. McGrory, E.C. Halbert, and P.W.M. Glaudemans, Phys. Lett. **26B**, 692 (1968).
[39] See Appendix A.1 in F. Petrovich, R.H. Howell, C.H. Poppe, S.M. Austin, and G.M. Crawley, Nucl. Phys. **A383**, 355 (1982).
[40] R.R. Whitehead, Nucl. Phys. **A182**, 290 (1972).
[41] R.R. Whitehead, in *Moment Methods in Many Fermion Systems*, edited by B.J. Dalton, S.M. Grimes, J.P. Vary, and S.A. Williams (Plenum, New York, 1979), p. 235; Bull. Am. Phys. Soc. **32**, 1012 (1987).
[42] S.D. Bloom, Prog. Part. Nucl. Phys. **11**, 505 (1984).
[43] D. Halderson, R.J. Philpott, J.A. Carr, and F. Petrovich, Phys. Rev. C **24**, 1095 (1981).
[44] J.A. Carr, F. Petrovich, D. Halderson, and J. Kelly, computer code ALLWRLD (unpublished).
[45] R.F. Hausman, Ph.D. thesis, LLNL publication UCRL-52178, 1976 (unpublished).
[46] S. Yen *et al.*, Phys. Lett. **93B**, 250 (1980).
[47] A. Fazely *et al.*, Nucl. Phys. **A443**, 29 (1985).
[48] N. Tamimi *et al.*, Phys. Rev. C **45**, 1005 (1992), this issue.
[49] G.S. Adams *et al.*, Phys. Rev. Lett. **38**, 1387 (1977).
[50] C. Olmer *et al.*, Phys. Rev. Lett. **43**, 612 (1979).
[51] S. Yen *et al.*, Phys. Lett. **105B**, 421 (1981).
[52] K. Hosono *et al.*, Phys. Rev. C **26**, 1440 (1982).
[53] G.T. Emery, A.D. Bacher, and C. Olmer, in *Spin Excitations in Nuclei*, edited by F. Petrovich *et al.* (Plenum, New York, 1984), p. 371.
[54] C. Olmer *et al.*, Phys. Rev. C **29**, 361 (1984).
[55] N.M. Hintz *et al.*, Phys. Rev. C **30**, 1976 (1984).
[56] S. Kato and K. Okada, J. Phys. Soc. Jpn. **50**, 1440 (1981).
[57] H. Nann, Nucl. Phys. **A376**, 61 (1982).
[58] K.A. Snover *et al.*, Phys. Rev. C **27**, 493 (1983).
[59] P.M. Endt and C. van der Leun, Nucl. Phys. **A521**, 1 (1990).
[60] J.A. Carr, F. Petrovich, D. Halderson, D.B. Holtkamp, and W.B. Cottingame, Phys. Rev. C **27**, 1636 (1983).
[61] J.A. Carr, S.D. Bloom, F. Petrovich, and R.J. Philpott, Phys. Rev. Lett. **63**, 916(C) (1989).
[62] D.F. Geesaman and B. Zeidman, Phys. Rev. Lett. **63**,

915(C) (1989).
[63] R.E. Segel *et al.*, Phys. Rev. C **39**, 749 (1989).
[64] B.D. Anderson, J.W. Watson, and R. Madey, in *Nuclear Structure at High Spin, Excitation, and Momentum (McCormick's Creek State Park, Bloomington, Indiana)*, Proceedings of the Workshop on Nuclear Structure at High Spin, Excitation, and Momentum Transfer, edited by H. Nann, AIP Conf. Proc. No. 142 (AIP, New York, 1986), p. 155.
[65] S. Yen, private communication concerning unpublished analysis of data from Ref. [46].
[66] A. Bacher, private communication.
[67] H. Zarek *et al.*, Phys. Rev. Lett. **38**, 750 (1977).
[68] H. Zarek *et al.*, Phys. Rev. C **29**, 1664 (1984).
[69] R.A. Lindgren *et al.*, Phys. Rev. C **44**, 2413 (1991).
[70] M.C. Munro *et al.*, IUCF Scientific and Technical Report, 1988, p. 15 (unpublished).
[71] B.D. Anderson *et al.*, Phys. Lett. **123B**, 383 (1983).
[72] K.W. Schmid, Phys. Rev. C **24**, 1283 (1981).
[73] B.S. Ishkhanov, I.M. Kapitanov, and A.V. Shumakov, Nucl. Phys. **A394**, 131 (1983).
[74] B.L. Clausen, R.J. Peterson, and R.A. Lindgren, Phys. Rev. C **38**, 589 (1988).
[75] R.J. Philpott, Nucl. Phys. **A289**, 109 (1977); D. Halderson and R.J. Philpott, *ibid.* **A321**, 295 (1979); **A345**, 145 (1980).

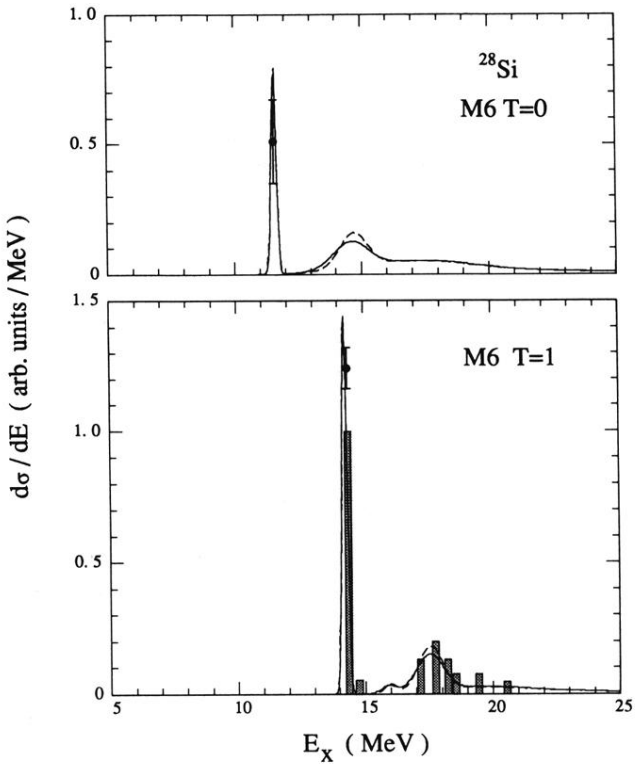

FIG. 1. Solid curves showing the predicted strength function for inelastic scattering to $T = 0$ (top) and $T = 1$ (bottom) 6^- states in ^{28}Si obtained with the $n_{\max} = 8$ basis are compared to "data points" (denoting the inelastic scattering results) and a histogram [denoting the (p, n) results] representative of the observed scattering strength. As discussed in the second half of Sec. II, the data points should be compared to the peak of the strength-function curve and the top of the histogram bar; the shaded area of the histogram also can be compared to the area under the strength-function curve. The dashed curve shows our earlier results [1] with the $n_{\max} = 4$ basis.

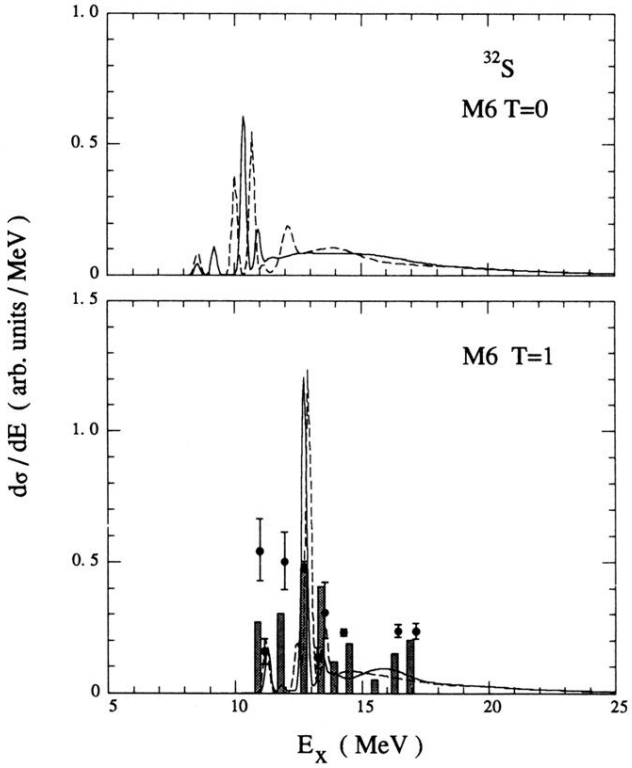

FIG. 2. Solid curves showing the predicted strength function for inelastic scattering to $T = 0$ (top) and $T = 1$ (bottom) 6^- states in ^{32}S obtained with the $n_{max} = 8$ basis are compared to "data points" [denoting (e, e') results] and a histogram [denoting (p, n) results] representative of the observed scattering strength. The dashed curve shows our earlier results [34] with the $n_{max} = 4$ basis.

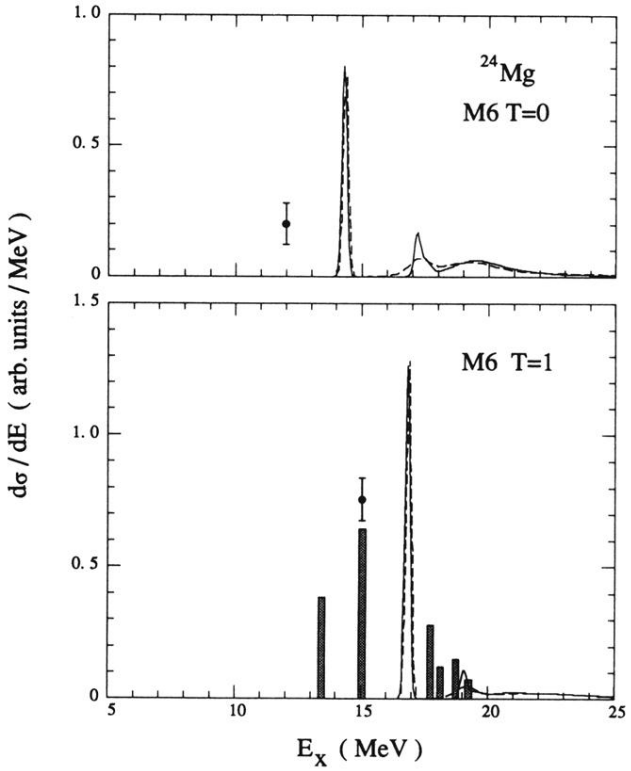

FIG. 3. Solid curves showing the predicted strength function for inelastic scattering to $T = 0$ (top) and $T = 1$ (bottom) 6^- states in ^{24}Mg obtained with the $n_{max} = 8$ basis are compared to "data points" (denoting inelastic scattering results) and a histogram [denoting the (p, n) results] representative of the observed scattering strength. The dashed curve shows results with the $n_{max} = 4$ basis.

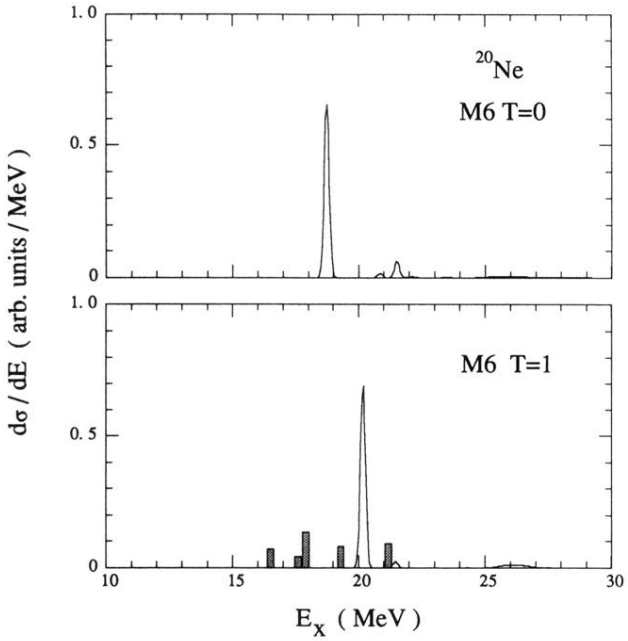

FIG. 4. Solid curves showing the predicted strength function for inelastic scattering to $T = 0$ (top) and $T = 1$ (bottom) 6^- states in ^{20}Ne obtained with the $n_{max} = 8$ basis are compared to a histogram representative of the scattering strength observed with the (p, n) reaction.